Dust as a tipping element: The Bodélé Depression, Chad

Richard Washington[a,1], **Christel Bouet**[b], **Guy Cautenet**[b], **Elisabeth Mackenzie**[a], **Ian Ashpole**[a], **Sebastian Engelstaedter**[a], **Gil Lizcano**[a], **Gideon M. Henderson**[c], **Kerstin Schepanski**[d], and **Ina Tegen**[d]

[a]Climate Research Lab, Centre for the Environment, University of Oxford, South Parks Road, Oxford OX1 3QY, United Kingdom; [b]Laboratoire de Météorologie Physique, Unité Mixte de Recherche, Centre National de la Recherche Scientifique 6016, Université Blaise Pascal, 63177 Aubière Cedex, France; [c]Department of Earth Science, University of Oxford, Parks Road, Oxford OX1 3PR, United Kingdom; and [d]Leibniz Institute for Tropospheric Research, 04318 Leipzig, Germany

Edited by Hans Joachim Schellnhuber, Potsdam Institute for Climate Impact Research, Potsdam, Germany, and approved March 24, 2009 (received for review December 17, 2007)

Dust plays a vital role in climate and biophysical feedbacks in the Earth system. One source of dust, the Bodélé Depression in Chad, is estimated to produce about half the mineral aerosols emitted from the Sahara, which is the world's largest source. By using a variety of new remote sensing data, regional modeling, trajectory models, chemical analyses of dust, and future climate simulations, we investigate the current and past sensitivity of the Bodélé. We show that minor adjustments to small features of the atmospheric circulation, such as the Bodélé Low-Level Jet, could profoundly alter the behavior of this feature. Dust production during the mid-Holocene ceased completely from this key source region. Although subject to a great deal of uncertainty, some simulations of the 21st century indicate the potential for a substantial increase in dust production by the end of the century in comparison with current values.

mineral aerosol | regional climate model | low-level jet

Mineral dust, as one of the most abundant aerosol species in the atmosphere (1), plays an important role in determining the heating of the planet. Single scattering albedo of dust largely controls the backscattering of solar radiation to space, but the influence of dust on the longwave-radiation budget is similar to greenhouse gases because of efficient absorption of the relatively large particle size characteristic of dust. The degree of absorption hinges mainly on the vertical profile of dust (2). As a result of these complexities, the sign and magnitude of the net radiative forcing of dust has the potential for high spatial and temporal variability (3). Local instantaneous direct radiative forcing effect, for example, has been measured in situ as 130 $W{\cdot}m^{-2}$ off the coast of West Africa (4), and a 50-$W{\cdot}m^{-2}$ longwave direct radiative dust effect over land areas of North Africa was measured for July 2003 (5).

Dust as a Tipping Element

Dust has been implicated in the activation and early growth of cloud droplets (6), in convection over the Atlantic (7), and in the reduction of the burden of anthropogenic species at sub-μm sizes, thereby limiting their residence time in the atmosphere (8). Dust interacts with a variety of large-scale circulation components, such as African easterly waves (9), with the potential to alter natural dust-source emissions through feedbacks. It has been argued that dust radiative forcing reduces the downward mixing of momentum within the planetary boundary layer and the surface-wind speed, thus reducing dust emission (10), a process which could decrease global dust load by 10–20%. Mineral aerosol deposition affects global ecosystems and processes, such as the biogeochemical cycle of the oceans, which requires Fe supplied by dust (11). Trace elements derived from dust emissions from a single part of the Sahara (12), for example, have also been proposed to be important in the Amazon basin (13), and phosphorus from Asian dust is argued to be vital to the Hawaiian Islands (14).

Recent satellite analyses have confirmed the importance of North African deserts in global dust production (15). Within this region, the Bodélé Depression in Chad stands out as a key emission source. Several factors earmark the Bodélé region as a potential tipping element, although the Bodélé has not, as yet, been independently considered a tipping element (16). First, the Bodélé may generate more than half the Sahara's mineral aerosol output (17, 18) (Fig. 1) and the accompanying impact on the Earth system. Second, it is a small, unvegetated depression (some 150 km × 150 km) lying only 200 km north of the contemporary monsoon rainfall limit (roughly one grid box in most global climate models) in the Sahara desert. Minor modifications to the global circulation could increase dust production from the Bodélé or else reduce it to near zero. There is evidence of such extreme variability during the Late Quaternary Period (19). During the Last Glacial Maximum, atmospheric dust concentration was as much as an order of magnitude more than present values (20). Observations suggest that annual mean African dust may have varied by a factor of 4 between 1960 and 2000 (21). With changes in aridity and circulation expected in forthcoming decades (22), it is likely that dust concentrations in the atmosphere will alter as well and that key dust sources like the Bodélé will play a central role in modulating this production.

This paper outlines the nature of the Bodélé source and provides reasons for its prominence. It goes on to evaluate the controls on Bodélé dust emission and the sensitivity of these controls, in part through multiple years of integration from 2 regional climate models. By using a Lagrangian trajectory model, we provide the first climatology of transport from the basin and present a chemical analysis of dust samples from the Bodélé compared with another key Saharan dust hotspot in Mali. We go on to provide a perspective of the basin's history during the Holocene before considering the possible behavior of the Bodélé in climate change simulations of the 21st century. We argue that the Bodélé is indeed capable of profound changes in future emissions. Although the full consequences of these change have not yet been quantified, the case exists for doing so.

Anatomy of the Bodélé Depression

Many studies have pointed to the Bodélé Depression as one of the key dust sources in the world (17, 23–27). Individual dust plumes from this source are clearly evident in MODerate Resolution Imaging Spectroradiometer (MODIS) true color imagery (28), occur ≈100 times per year, average 370 km × 700 km in area, carry 700,000 tons of sediment, and are responsible

---

Author contributions: R.W., C.B., G.C., E.M., I.A., S.E., G.L., G.M.H., K.S., and I.T. performed research; and R.W., C.B., and G.C. wrote the paper.

The authors declare no conflict of interest.

This article is a PNAS Direct Submission.

[1]To whom correspondence should be sent. E-mail: richard.washington@ouce.ox.ac.uk.

www.pnas.org/cgi/doi/10.1073/pnas.0711850106

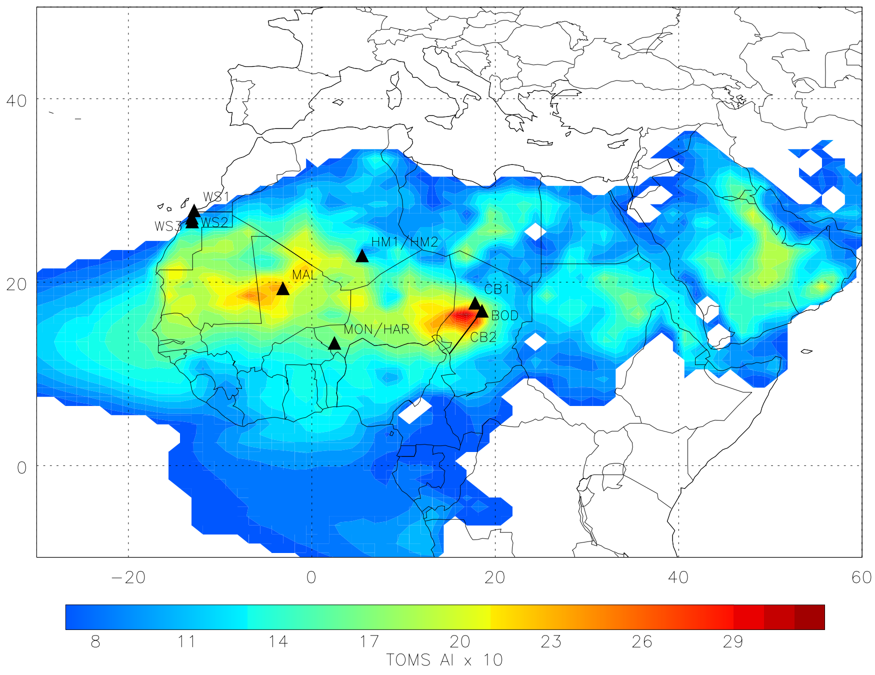

Fig. 1. TOMS AI annual average 1979–1992 for North Africa. Sample locations from Table 1 also shown. BOD, Bodélé; CB1-2, Chad Basin; HAR, Harmattan; HM1-2, Hoggar Massif; MAL, Mali; MON, monsoon; WS1-3, Western Sahara.

for up to 40% of the Aerosol Optical Thickness (AOT) over the equatorial Atlantic and Amazon basin (12).

Two key components are required for such extensive deflation, namely extensive, highly erodible sediments and a colocated erosive wind. The Bodélé Dust Experiment (BoDEx) (29, 30) confirmed that the MODIS dust plumes originate from a shallow basin of exposed diatomite sediment, much of which was deposited under paleolake Megachad some 7,000 years ago when it was the biggest lake on the planet (19). This silicious, low-density, and highly friable material covers ≈10,800 km^2 of the basin. The northeastern portion of the depression is being invaded by large barchans dunes (some more than 1 km from horn to horn) that are composed of silt-sized diatomite pellets. The northern part of the basin is underlain by diatomite slabs ≈1 m in diameter. Toward the central and southern parts of the basin, the diatomite is broken into pellets of a few cm or less in diameter.

The wind responsible for deflating the diatomite has been identified as the Bodélé low-level jet (LLJ) (26) which is part of the northeasterly Harmattan flow. It is accelerated between the topography of the Tibesti mountains and the Ennedi ridge to reach a low-level wind speed maximum ≈200 m above the surface of the basin. The LLJ is absent in the time-mean flow at other longitudes across the Sahara. Regional modeling studies show that the presence of the topography accelerates the wind by ≈40% (31). Pilot balloon measurements during BoDEx point to a marked diurnal cycle in the wind speed such that the LLJ accelerates over a near frictionless inversion by night but is mixed down to the surface by extreme radiative heating through modification of eddy viscosity to produce a surface-wind-speed maximum by ≈1100 local time (32).

Controls on Dust Emission

One way of assessing the sensitivity of the Bodélé as a tipping element is to evaluate the controls on the variability of the erodibility and erosivity components that determine deflation. If it can be shown that Bodélé dust emission is subject to strong modulation on a variety of time scales that influence the overall output of dust, then insights into the thresholds which constrain the system may be gained. These controls are discussed in this section on time scales ranging from the diurnal to the annual cycles and to the long-term behavior during the Holocene.

Contemporary Controls

Dust emission from the Bodélé is strongly modulated on a diurnal cycle. Composites of surface-wind speed from both dusty and dust-free days measured during BoDEx featured a strong diurnal amplitude (0–6 m/s^{-1} on dust-free days, 4–13 m/s^{-1} on dust-emission days) with an early-evening minimum near 2100 local time and a midmorning maximum near 1100 local time. Although MODIS satellites only pass twice daily and cannot therefore be used to determine the diurnal cycle of dust emission directly, analyses of imagery from this satellite have shown that distinct packages of dust plumes are traceable for several days downwind of the Bodélé, indicating that large-scale emissions are strongly modulated by the diurnal cycle (28). Recently available data at 15 min time resolution derived from the geostationary Meteosat Second Generation satellite's Spinning Enhanced Visible and Infrared Imager has been used to analyze Saharan dust (33). The spatial Dust Source Activation Frequency emerging from this work has been applied to the Bodélé Depression (Fig. 2) where activation was found to occur on 65% of all days. In all months, the diurnal peak in onset of emissions is very clearly between 0700 and 1000 local time, followed by the previous or subsequent 3-h period on a monthly dependent basis. Minimum dust emission occurs in the evening. This data, although only analyzed for 17 months, corroborates other satellite and field data, enforcing the view that dust emissions are transport-limited by the pulsing of the surface wind. A key control of Bodélé dust output is therefore the behavior of the Bodélé LLJ, which ranges naturally within and beyond the threshold required for deflation.

On a day-to-day basis, the strength of the Bodélé LLJ is modulated by the ridging of the Libyan high-pressure system (LHPS) (26) which has the effect of raising surface winds above the threshold for deflation of ≈10m/s^{-1} (34). The LHPS enhances the pressure gradient, causing acceleration in the flow

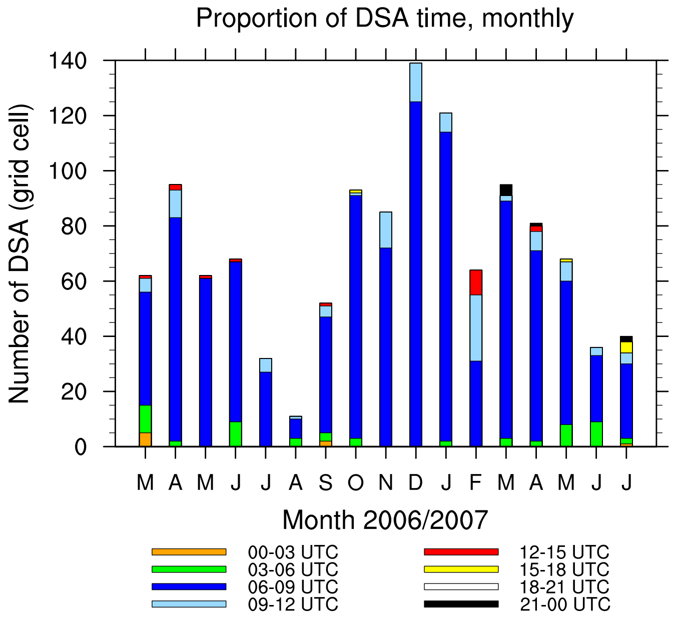

Fig. 2. Diurnal [in 3-h categories 00–03 universal time coordinated (UTC), etc.] and annual cycles of dust-source activation frequency over the Bodélé, March 2006 to July 2007.

that typically lasts 1–3 days between the Tibesti and Ennedi topography. The flow is ageostrophic, possibly resulting from density currents consequent on large-scale evaporation at the leading edge of the ridging anticyclone (35). The association between the synoptic forcing of dust events and the role of the Bodélé LLJ has been verified here by running a regional model for all large-scale dust events (established from plumes deflating from the Bodélé in MODIS imagery) (32) from January to March between 2002 and 2005 by using the Fifth Generation National Center for Atmospheric Research/Penn State Regional Mesoscale Meteorological Model, Version 5 (MM5) previously set up for the Bodélé domain (31). Composites of these events for each of the months have been studied. In all cases, the Bodélé LLJ was enhanced in MM5 by 3 to 4 m/s^{-1} above the daily mean (Fig. 3) and occurred in conjunction with a ridging anticyclone through Libya.

Satellite-derived dust-emission data [e.g., Total Ozone Mapping Spectrometer (TOMS), AOT, MODIS] used to quantify the annual cycle in the Bodélé point to a minimum in Bodélé dust emissions from June to September and a maximum between December and March (32). An exception is the TOMS aerosol index (AI) data, which places the maximum during May. This exception may be the result of a bias inherent in the TOMS AI definition that makes the index sensitive to the altitude of the dust layer. Deflation is still active in May, but surface heating is near a peak during this month given the low cloudiness and the near-zenith position of the sun. The combination of intense convection and surface dust may loft dust to midlevels where the TOMS AI bias results in a peak in detection. In cooler months, when convection is less intense, the dust stays close to the surface and may consequently be underestimated by TOMS AI.

Dust emissions from the Regional Atmospheric Modeling System (RAMS) (36) coupled online with the Dust Production Model (37–40) have been calculated for 2001 by using a horizontal resolution of 50 km both in *x* and *y* directions over 0 °E to 27 °E and 12 °N to 27 °N with 30 vertical levels from ground to 22 km, including 12 levels from surface to 1.2 km. The simulation emulates the annual cycle of dust derived from the Infrared Difference Dust Index (IDDI) (41) satellite product

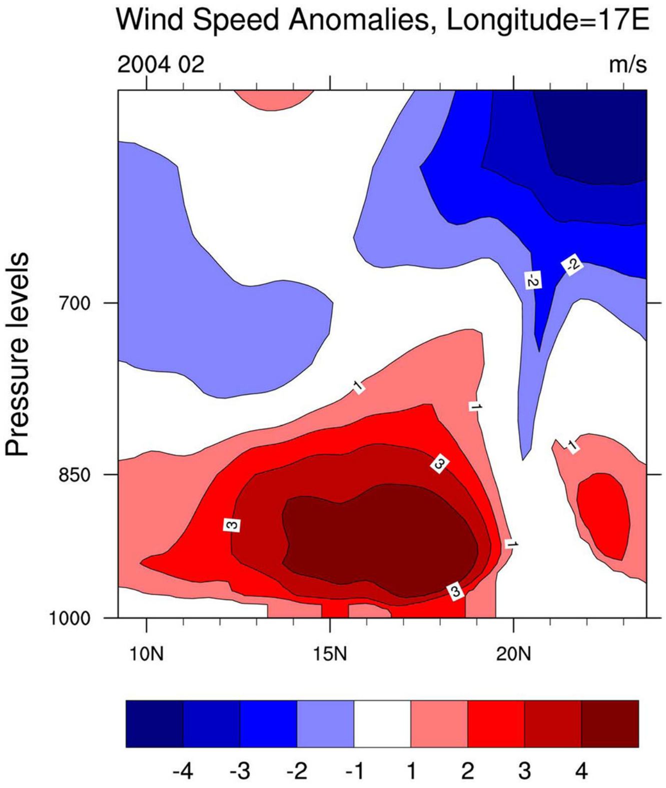

Fig. 3. Wind-speed anomalies (latitude vs. height) in m/s from MM5 regional model integrations for major Bodélé dust plume events in February 2004.

reasonably well, with a maximum in dust concentration in winter and a minimum in summer (Fig. 4). Moreover, the phase of the annual cycle of observed surface-wind speed (at Faya-Largeau, 18 °N, 19 °E) is fairly well reproduced by RAMS, whereas it is quasiinexistent in the reanalysis data (Fig. 5). This result again reinforces the important control imposed by the Bodélé LLJ.

To understand the modulation of the annual cycle better, the surface-wind flux *WF*, taken as the airflow entering the defile between the Tibesti and the Ennedi mountains across a control surface oriented northwest to southeast, with a horizontal width of 250 km and a height of 50 m, has been computed from the RAMS regional model for 2001 as follows:

$$WF = \iint_{(\Sigma)} \vec{V} \cdot \vec{n} d\sigma$$

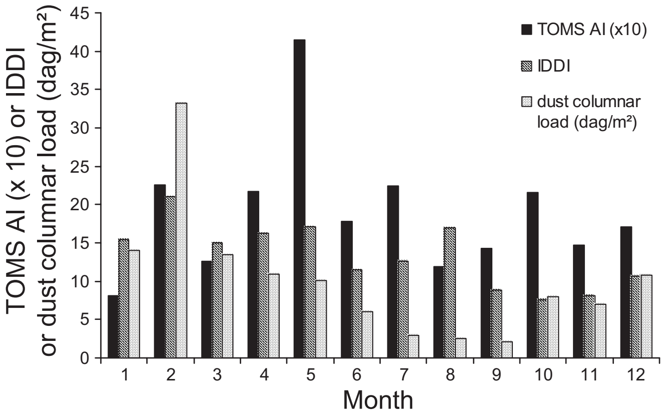

Fig. 4. Annual cycle of Bodélé dust as estimated from TOMS AI, IDDI, and the RAMS dust columnar loading.

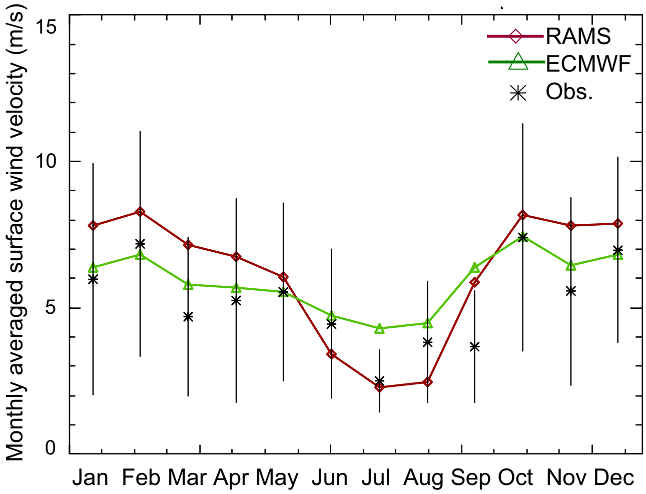

Fig. 5. Monthly mean values of surface-wind velocity as measured at Faya (18 °N; 19 °E) meteorological station (black stars) and as modeled by the European Centre for Medium-Range Weather Forecasts (ECMWF) global model (green triangles) and the mesoscale RAMS model (red diamonds) for 2001. Vertical bars represent the standard deviation.

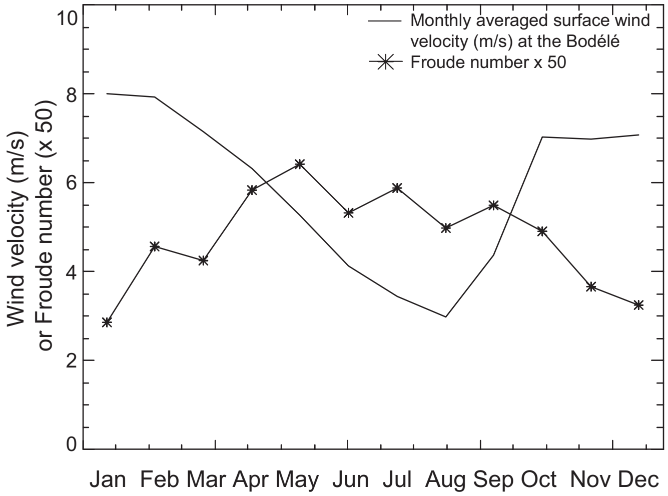

Fig. 7. Monthly mean values of the modeled (RAMS) surface-wind velocities (in m/s) at the Bodélé (solid line) and Froude number (×50; stars) for 2001.

where $\vec{V}$ is the wind vector and $\vec{n}$ is the unit vector normal to surface $d\sigma$.

A negative *WF* value (wind direction from northeast to southwest, as is the case in winter), is associated with high surface-wind velocity over the Bodélé dust-source area, and therefore intense dust emissions. On the other hand, when wind direction is reversed (positive *WF*) acceleration through the venturi no longer exists, and surface-wind velocity rarely exceeds the wind threshold necessary for dust emission (Fig. 6). The nondimensional Froude number representing flow's ability to overpass an obstacle, *Fr*, has also been computed from the RAMS data for negative *WF* cases as follows:

$$Fr = \frac{U}{Nh}$$

where U is the mean wind velocity and N is the Brünt-Väisälä frequency. In the present study, h is the order of magnitude of the Tibesti Mountain. Only the relative variations of *Fr* (because the barrier is finite and the absolute variability of *Fr* is consequently not applicable) with wind speeds are considered (Fig. 7). When the *Fr* value is lower, airflow is forced into the venturi and the flow accelerates.

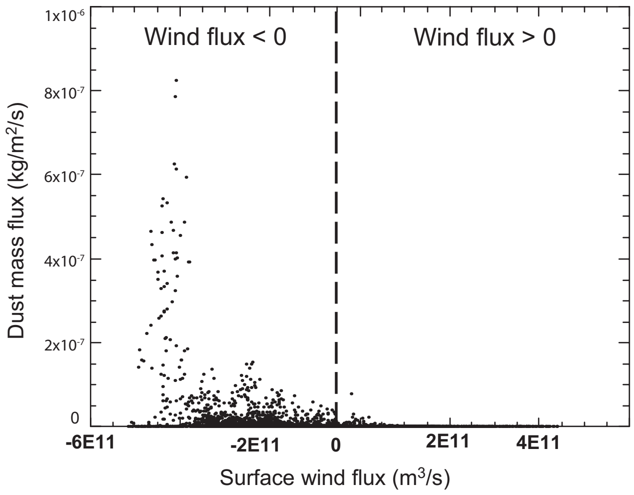

Fig. 6. Modeled (RAMS) dust mass flux (in kg/m^{-2}/s^{-1}) as a function of modeled surface-wind flux (m^3/s^{-1}) for 2001.

It is clear from the analysis of contemporary controls on Bodélé dust emission on time scales ranging from the diurnal to the annual that erosivity in the form of the Bodélé LLJ currently modulates dust emission. Whether or not erodibility factors also exert an influence needs to be established by considering longer time scales.

Holocene

Considerable evidence suggests that paleolake Megachad was the world's largest lake sometime before 7,000 years ago (19, 42, 43). Intercalation of diatomites and dune sands in the northeastern Bodélé show that this lake has filled and emptied ≥3 times during the last 3,000 to 4,000 years. Diatomite was deposited when the lake was filled; in dry periods, quartz sand dunes driven in by the northeasterly Bodélé LLJ invaded the lakebed as they are again doing at present (19, 31). Erodibility places key limitations on the long-term behavior of the Bodélé. Reversion to wetter conditions indicates a shutdown in dust production from this key source, accompanied by lower atmospheric optical depths across West Africa and the Atlantic.

It has been argued that the cycle of wetting and drying in the Bodélé forms an important component in the operation of this tipping element (31) beyond simply a relaxation in deflation in wetter times followed by deflation in drier times. Climate model simulations of the Last Glacial Maximum show an even stronger Bodélé LLJ compared with that of the present, and dated evidence points to the conditions under which deflation would have been capable of excavating the depression which was later partly filled by paleolake Megachad (31). Importantly, the lake was subsequently populated by the diatomite material which is currently being deflated. It follows that a combination of atmospheric, hydrological, and geomorphological processes in the past have been responsible for maintaining and intensifying what is now the greatest dust source on Earth, and this process necessarily entails periods during which no deflation occurs. In this sense, the Bodélé has remarkable capacity as a potential tipping element. Periods of low deflation are simply important opportunities for recharge of the erodible sediment.

Table 1. Key major element oxide concentrations for new Bodélé and Mali samples in comparison with other Saharan dust samples

Element Oxide Concentrations	HM1	HM2	CB1	CB2	Bod	MON	HAR	WS1	WS2	WS3	Mal
Al_2O_3	14.73	13.59	13.97	11.65	11.65	11.61	12.16	8.79	7.01	5.08	4.49
Fe_2O_3	6.06	5.17	6.71	4.7	5.60	4.38	5.69	4.37	2.8	4.22	1.65
MgO	1.76	1.55	1.21	0.76	0.79	0.47	0.9	2.88	2.58	1.91	2.58
CaO	2.43	2.01	1.39	1.42	0.34	0.36	1.64	12.88	17.65	12.21	26.44
Na_2O	1.63	1.92	1.05	0.45	2.17	0.35	0.6	0.94	0.73	0.82	0.41
K_2O	2.49	2.46	1.47	1.51	1.22	1.19	1.77	1.94	1.66	1.35	0.79
P_2O_5	0.29	0.24	0.22	0.15	0.21	0.1	0.15	0.17	0.39	0.45	0.29

Units are wt % oxide. Sample locations are shown in Figure 1. HM1-2, Hoggar Massif; CB1-2, Chad Basin; BOD, Bodélé; MON, monsoon; HAR, Harmattan; WS1-3, Western Sahara; MAL, Mali.

Contemporary Dust Chemistry and Transport

A vital component of diagnosing the role of the Bodélé in the Earth system rests on its contribution to biogeochemical cycling. Although measurements of aerosols from airborne work (e.g., ref. 44) and land-based and shipboard filter systems (e.g., ref. 45) all point to the spatial variability of aerosol chemistry, these techniques sample a mixture of aerosols from different regions. The chemistry of the individual source regions has not been extensively investigated. An exception is a geochemical study of 9 source samples, including 2 samples from the Bodélé Depression (Table 1) (46). We augment this data with major element compositions for 2 new samples—one from the Bodélé Depression, and, for comparison, one from the unsampled and extremely remote Taoudeni Basin that spans much of Northern Mali. The Taoudeni Basin represents a distinct geological environment from other North African dust sources and consists of an extensive Lower Paleozoic sedimentary sequence that includes frequent carbonate units (47). The sample derives from a hotspot of dust in West Africa (near 19.5 °N, 3.125 °E) that represents the second most significant dust source in the Sahara (48).

The Bodélé source region chemistry reflects weathered average continental crust. The major-element chemistry of these 3 samples (Table 1) is similar despite differing local settings of collection, probably as a result of mixing of source material on the land surface. Al_2O_3 and Fe_2O_3 contents are typical for upper continental crust with Fe/Al ratio of 0.40–0.48. Content of more soluble elements (e.g., Ca, Mg, Na) are lower than in average continental crust, probably because of the absence of sedimentary carbonates in the region. The Bodélé sample chemistry is in marked contrast to that the Taoudeni Basin. That sample has Al_2O_3 and Fe_2O_3 contents about one-third those of average continental crust but with significantly higher CaO concentration, reflecting frequent carbonate rocks in this area.

We have computed the transport pathways from the Bodélé Depression by using a Lagrangian advection model driven by 3-dimensional ERA-40 reanalysis winds. Twenty-five forward trajectories were released every 6 h from a region overlying the depression (17 °N, 18 °E) for the period from January 1970 to December 1999, and the parcel positions were noted for each 6-h period for 4 days after release. The median path of the trajectories (Fig. 8) in the peak dust-production months reaches the Atlantic in just under 5 days. During the summer, when dust production is much lower, the transport pathway is over West Africa in the core of the African Easterly Jet. The sediment that is deflated in this season then augments the material derived from the key summertime sources over Mali and Mauritania.

The chemistry of the mineral dusts from these source regions has a significant impact on biogeochemical cycles in the Atlantic Ocean (49). Fe is an essential nutrient for ocean ecosystems, and its supply limits the productivity of large areas of the modern ocean (11). Supply of new Fe to surface waters of the open Atlantic is thought to be dominated by dissolution of mineral aerosols (11), as is clearly seen by using dust-sourced Al as a tracer of Fe supply even after rapid biological consumption of Fe (50). Variation in the supply of dust from North African sources therefore has potential to cause significant changes in the size and function of ocean ecosystems across much of the Atlantic basin. The extent of present-day primary Fe limitation in the

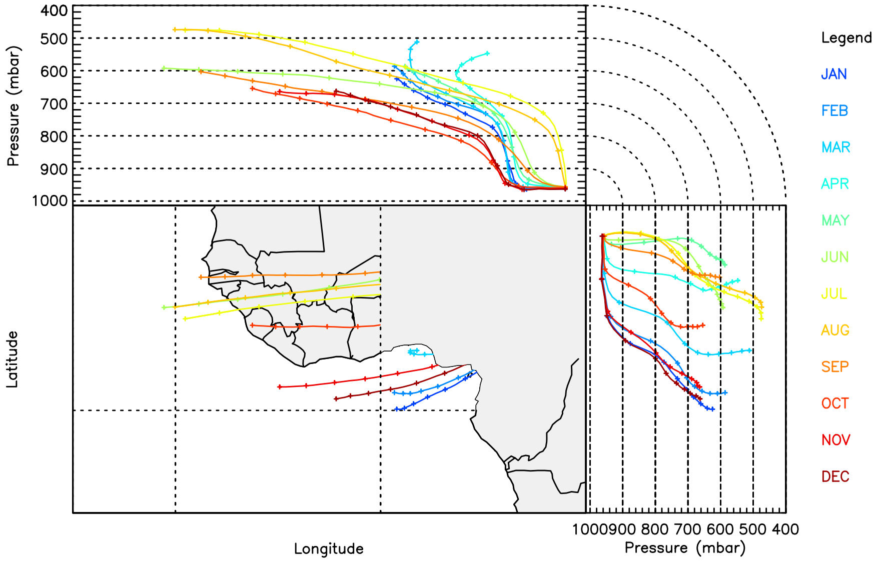

Fig. 8. Median annual cycle of 10-day trajectories from the Bodélé, January 1970 to December 1999.

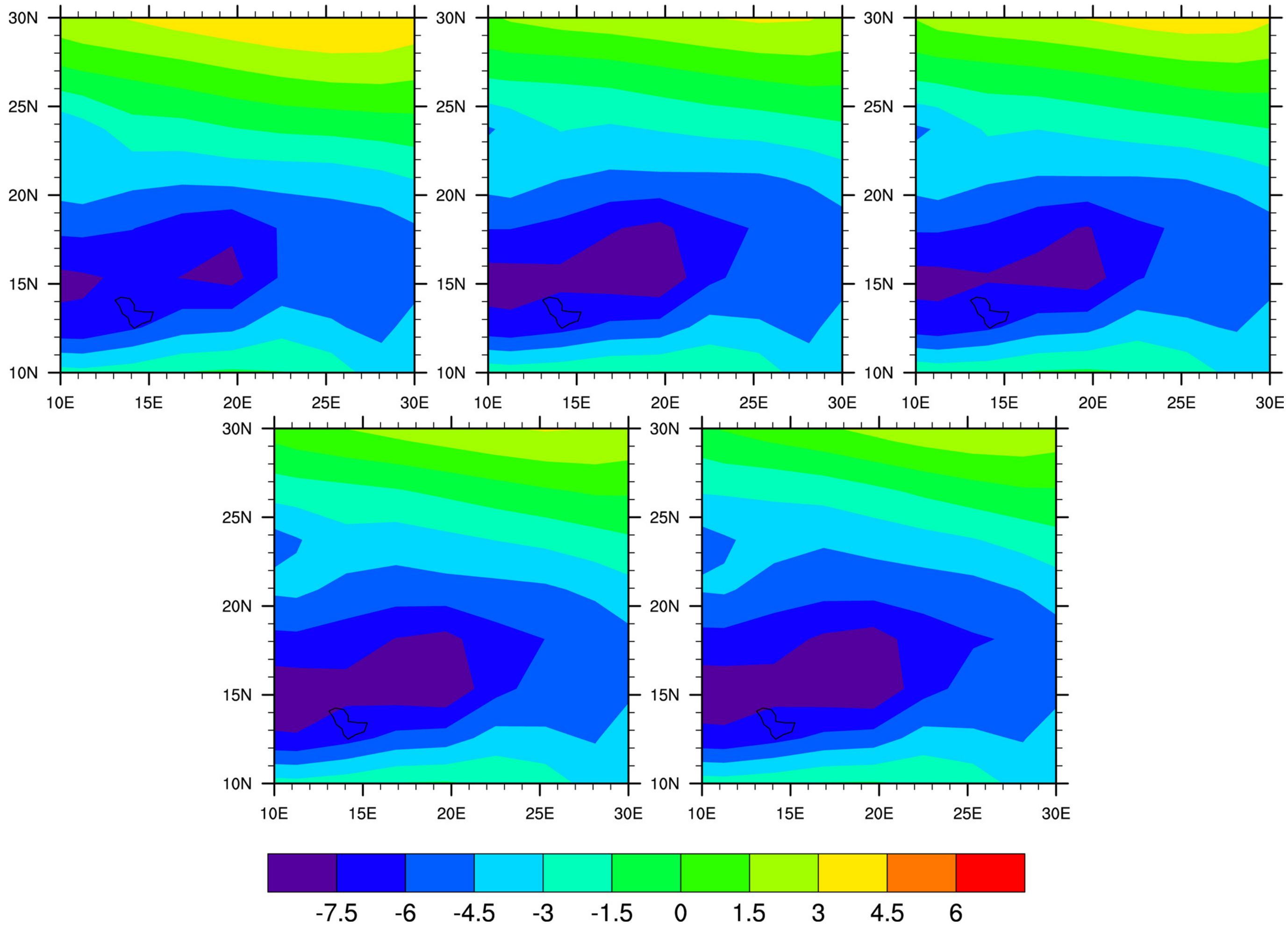

Fig. 9. Zonal 925-hectopascal (hPa) winds in m/s from the MRI model for January to March over the Bodélé for 1991–2000 (*Upper Left*), 2046–2055 (*Upper Middle*), 2056–2065 (*Upper Right*), 2081–2090 (*Lower Left*), 2091–2100 (*Lower Right*).

Atlantic remains a matter of debate (51), suggesting that the system is poised relatively close to Fe limitation and may be sensitive to change of Fe inputs, particularly to decreases in supply. Fe supply is important even in regions directly under the Saharan dust plume (shown in the trajectory analysis to be augmented by Bodélé dust) where, although primary Fe limitation is unlikely, the supply of Fe exerts a secondary control on ocean productivity because it is required for the fixation of nitrogen, the main limiting nutrient in these areas (52). This secondary role suggests that even an increase of dust input to further reduce primary Fe limitation may have important implication for Atlantic ecosystems and carbon cycling.

North African mineral dust also exerts considerable influence on tropical landmasses east of the Atlantic. Saharan dust is the primary source of mineral material in soils in many areas of the Caribbean, and impacts corals reefs in the area through both particulate and chemical supply (53). The Bodélé Depression is particularly important in the supply of mineral dust to the Amazon region during winter when the Bodélé source is at its strongest (27). Although the median trajectories fail to reach the Amazon within 10 days, some 10% of parcel trajectories in the December to May season do. This vector may be a significant and time-varying source of nutrients to the Amazon rainforest. There is clear evidence that the supply of mineral dust to the tropical western Atlantic region has been controlled by environmental conditions in the Saharan region during the 20th century (21) with increases in dust supply linked to increased aridity since 1970. Such changes in dust supply have the potential to significantly alter biogeochemical cycles, to impact Atlantic open-ocean ecosystems, Caribbean coral reefs, and the Amazon rainforest. It is clear from the analysis of Holocene conditions in the Bodélé that for extended periods this supply of nutrients was nonexistent. Quantification to determine whether or not the dust flux constitutes a true tipping element is yet to be established, but the case exists for assessing its role.

Bodélé Future

The Bodélé Depression has undergone profound changes during the Holocene. Its current dust output is essentially transport-limited, but with expected changes in future atmospheric circulation in response to increasing greenhouse gas concentrations, changes to deflation in the Bodélé may impose critical changes on the behavior of the Earth system in response to the role that dust plays in the biosphere and the sheer quantity emitted from this key region.

An extensive set of model integrations available from the Program for Climate Model Diagnosis and Intercomparison for the Fourth Assessment Report of the Intergovernmental Panel on Climate Change (IPCC AR4) have been analyzed over the 21st century for West Africa (54, 55) to assess the likely future climate in this key region. The models reported in the IPCC AR4 disagree about future rainfall in the Sahel, with some suggesting wetter future conditions and some drier (54). The coarse resolution of global models, together with regional uncertainties in precipitation, make it difficult to assess the probability of deflation becoming supply-limited consequent on wetting of the Bodélé and/or increased vegetation cover over the basin. Clearly this cannot be ruled out, and, if it were to occur, the Bodélé may enter one of the replenishment phases. Based on a sample of 10 leading IPCC AR4 models (CNRM, CSIRO, GISS, MIUB, HadGEM, CCCMA, GFDL, ECHAM5, MRI, HadCM3), 4 models show that, in comparison with 1971–2000, more rainfall over the Bodélé is likely for the last decade of the 21st century, whereas 6 show that drier conditions are likely. The ensemble mean is for wetter conditions. The wettest model (>70–100 mm by 2100) shows an increase in rainfall in the early decades of the 21st century but also shows decades that are drier than present. Given that the ensemble mean temperature is projected to rise by 4–5 °C by 2100 in this region, evaporation will rise considerably too. From this perspective, the model projections suggest that rainfall increases would not be sufficient to support sufficient vegetation to stop dust emission. With a larger increase in rainfall (approximately >300–400 mm), dust production from the world's premier aerosol source would be reduced considerably and could plausibly cease altogether, with concomitant consequences for the Earth system in terms of nutrient supply to both terrestrial and oceanic ecosystems and the direct and indirect impact on the radiative balance.

Of the 10 models considered, 8 show an increase in mean annual surface-wind speed by the last decade of the 21st century compared with 1971–2000, and all 10 show an increase from January to March (JFM) (max, +0.8m/s^{-1}; min, +0.2 m/s^{-1}). Choosing only those models with a realistic simulation of the current climate, the selection is limited to 3 models, 2 of which, Meteorological Research Institute (MRI) and Geophysical Fluid Dynamics Laboratory (GFDL), show dry conditions over the Sahel during the 21st century (55). We analyze the daily MRI circulation fields in detail for the Special Report on Emissions Scenarios (SRES A2) scenario over the Bodélé, as regional drying in this model denotes that surface winds will remain the primary influence on dust emissions from this arid region. MRI is also suitable for this study because it demonstrates good skill in reproducing the Bodélé LLJ characteristics over the focus region of Northern Chad.

Near-surface zonal winds over the Bodélé Depression in MRI enhance considerably during the course of the 21st century based on decadal means. In the decade 1991–2000, easterly winds exhibit an average peak speed of 9 m/s^{-1} within the core of the jet, extending from 15–17 °N, 17–20 °E and fragmenting over Lake Chad. By 2091–2100 the spatial coverage of the LLJ has increased, extending from 3–21 °E across the region with a clear focus of expansion over the Bodélé (Fig. 9). Decadal variability in the wind strength is evident (e.g., diminished winds from 2056–2065 relative to the previous decade), but this is to be expected given the natural decadal and multidecadal fluctuations inherent to the climate of North Africa.

Because dust mobilization arises from synoptic-scale events in the Bodélé, the extremes of daily wind-speed distribution and their frequency of occurrence in each month are crucial components in modeling dust output. Although the shape of wind-speed distribution remains relatively constant through the decades, peaking between 11–13 m/s^{-1}, the frequency of winds stronger than 10 m/s^{-1} (a rough threshold for deflation in the basin) is markedly greater in the latter half of the 21st century (Fig. 10). The percentage of JFM days with winds exceeding 11 m/s^{-1} increases from 45% (1991–2000) to 49% (mid-21st century), exceeding 56% by the end of the century. The Bodélé winds show a doubling in the number of February days with wind speeds exceeding 11m/s^{-1} by the end of the century (all increases at or better than $P = 0.05\%$).

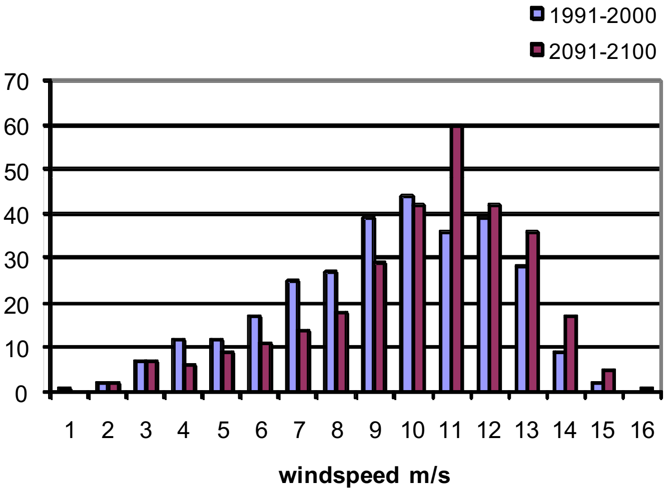

Fig. 10. Histogram (frequency of occurrence on vertical axis vs. wind speed on horizontal axis) of JFM Bodélé 925-hPa winds in m/s for 1991–2000 and 2091–2100 from the MRI model.

Bodélé LLJ strength correlates with shifts in the pressure gradient driving the northeasterlies, originating from a ridging of the LHPS (26). An increased strength of this LHPS is recognized in the JFM vector wind differences between the decades 1991–2000 and 2091–2100, which exhibit a strengthening of northeasterlies driving over the Libya–Chad border across the leading edge of the depression (Fig. 11). Almost identical results emerge from the Model for Interdisciplinary Research on Climate (MIROC) model for the same sampling base. Taken together, it is clear that large-scale adjustments to the general circulation are capable of increasing Bodélé winds in these models when forced with the A2 SRES scenario. Given the cubic sensitivity of dust mobilization to wind speed, these results point to the possibility of a substantial increase in dust output from the world's largest mineral aerosol source toward the end of the 21st century.

Summary

Several factors distinguish the Bodélé as a potential tipping element. It is the largest single source of mineral dust on the

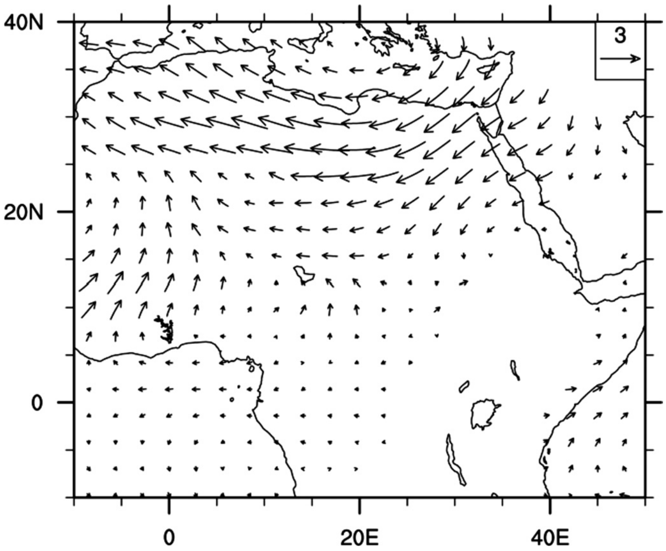

Fig. 11. JFM Bodélé 925-hPa vector wind differences for 1991–2000 and 2091–2100 from the MRI model. Vector shows 3 m/s.

planet, producing about half of the Sahara's mineral aerosol loadings. Mineral dust plays a key role in modifying climate through interaction with cloud physics and radiative heating. It is also involved in numerous biophysical feedbacks both in the oceans and on land. The Bodélé is, nevertheless, a very small region, and the controls on deflation are sensitive to changes in both erosivity and erodibility. Deflation is currently transport-limited and is extremely sensitive to a small-scale atmospheric feature in the form of the Bodélé LLJ. The critical parameters controlling large-scale deflation are known. Modulation of the surface-wind strength in response to the jet characteristics currently exerts a profound control on the output from the depression. Modulation of the jet on diurnal to annual cycles provides a clear demonstration of this sensitivity. On longer time scales, adjustments to the global circulation over the last 7,000 years have, during wetter times, reduced deflation from the depression to zero. But during these times, the material which is currently being deflated is replenished. The Bodélé may revert to such a state toward the end of the 21st century, and the transition times may be very short—as little as one season. On the other hand, some climate model simulations suggest that on these time scales the dust output from the basin may increase substantially. The full impacts of Bodélé dust on the Earth system are as yet unknown. The Bodélé, at this stage, qualifies as a potential tipping element until more work can be done to quantify the radiative impacts and biogeochemical consequences of mineral aerosols.

ACKNOWLEDGMENTS. We thank Chris Scott (www.sahara-overland.com) for collecting the sediment sample in a remote part of Mali. RAMS modeling was supported by the national program Chimie Atmosphérique, a part of the Les Enveloppes Fluides et l'Environnement national program.

1. Penner JE, et al. (2001) *Climate Change 2001: The Scientific Basis*, eds Houghton J, et al. (Cambridge Univ Press, Cambridge, UK).
2. Tanre D, et al. (2003) Measurement and modeling of the Saharan dust radiative impact: Overview of the Saharan Dust Experiment (SHADE). *J Geophys Res*, 10.1029/2002JD003273.
3. Miller RL, Tegen I (1998) Climate response to soil dust aerosols. *J Clim* 11:3247–3267.
4. Haywood J, et al. (2003) Radiative properties and direct radiative effect of Saharan dust measured by the C-130 aircraft during SHADE: 1. Solar spectrum. *J Geophys Res* 108:8577.
5. Haywood JM, et al. (2005) Can desert dust explain the outgoing longwave radiation anomaly over the Sahara during July 2003? *J Geophys Res*, 10.1029/2004JD005232.
6. McFiggans G, et al. (2006) The effect of physical and chemical aerosol properties on warm cloud droplet activation. *Atmos Chem Phys* 6:2593–2649.
7. Koren I, Kaufman YJ, Rosenfeld D, Remer LA, Rudich Y (2005) Aerosol invigoration and restructuring of Atlantic convective clouds. *Geophys Res Lett*, 10.1029/2005GL023187.
8. Bauer SE, Koch D (2005) Impact of heterogeneous sulfate formation at mineral dust surfaces on aerosol loads and radiative forcing in the Goddard Institute for Space Studies general circulation model. *J Geophys Res* 110:D17202.
9. Jones C, Mahowald N, Luo C (2004) Observational evidence of African desert dust intensification of easterly waves. *Geophys Res Lett* 31:L17208.
10. Miller RL, Perlwitz J, Tegen I (2004) Feedback upon dust emission by dust radiative forcing through the planetary boundary layer. *J Geophys Res* 109:D24209.
11. Jickells TD, et al. (2005) Global iron connections between desert dust, ocean biogeochemistry, and climate. *Science* 308:67–71.
12. Koren I, et al. (2006) The Bodélé Depression: A single spot in the Sahara that provides most of the mineral dust to the Amazon forest. *Environ Res Lett* 1:014005.
13. Okin GS, Mahowald N, Chadwick OA, Artaxo P (2004) Impact of desert dust on the biogeochemistry of phosphorus in terrestrial ecosystems. *Global Biogeochem Cycles* 18:GB2005.
14. Chadwick OA, Derry LA, Vitousek PM, Huebert BJ, Hedin LO (1999) Changing sources of nutrient during four million years of ecosystem development. *Nature* 397:491–487.
15. Prospero JM, Ginoux P, Torres O, Nicholson SE, Gill TE (2002) Environmental characterization of global sources of atmospheric soil dust identified with the Nimbus 7 Total Ozone Mapping Spectrometer (TOMS) absorbing aerosol product. *Rev Geophys* 40:1002.
16. Lenton TM, et al. (2008) Tipping elements in the Earth's climate system. *Proc Natl Acad Sci USA* 105:1786–1793.
17. Washington R, Todd MC, Middleton N, Goudie AS (2003) Dust-storm source areas determined by the Total Ozone Monitoring Spectrometer and surface observations. *Ann Assoc Am Geogr* 93:297–313.
18. Goudie AS, Middleton NJ (2001) Saharan dust storms: Nature and consequences. *Earth-Sci Rev* 56:179–204.
19. Drake N, Bristow C (2006) Shorelines in the Sahara: Geomorphological evidence for an enhanced monsoon from paleolake Megachad. *Holocene* 16:901–911.
20. Harrison SP, Kohfeld KE, Roelandt C, Claquin T (2001) The role of dust in climate changes today, at the last glacial maximum and in the future. *Earth-Sci Rev* 54:43–80.
21. Prospero JM, Lamb PJ (2003) African droughts and dust transport to the Caribbean: Climate change implications. *Science* 302:1024–1027.
22. Meehl GA, et al. (2007) in *Climate Change 2007: The Physical Science Basis*, eds Solomon S, et al. (Cambridge Univ Press, Cambridge, UK).
23. Herman JR, et al. (1997) Global distribution of UV-absorbing aerosols from Nimbus7/TOMS data. *J Geophys Res* 102:16911–16922.
24. Brooks N, Legrand M (2000) Dust variability over Northern Africa and rainfall in the Sahel. *Linking Climate Change to Land Surface Change*, eds McLaren S, Kniveton D (Kluwer Academic Publishers, Dordrecht), pp 1–26.
25. Middleton NJ, Goudie AS (2001) Saharan dust: Sources and trajectories. *Trans Inst British Geographers* 26:165–181.
26. Washington R, Todd MC (2005) Atmospheric controls on mineral dust emission from the Bodélé Depression, Chad: The role of the Low Level Jet. *Geophys Res Lett* 32:L17701.
27. Washington RM, Todd C, Middleton N, Goudie AS (2003) Dust-storm source areas determined by the total ozone monitoring spectrometer and surface observations. *Ann Assoc Am Geogr* 93:297–313.
28. Koren I, Kaufman YJ (2004) Direct wind measurements of Saharan dust events from Terra and Aqua satellites. *Geophys Res Lett* 31:L06122.
29. Tegen I, et al. (2006) Modelling soil dust aerosol in the Bodélé depression during the BoDEx campaign. *Atmos Chem Phys* 6:4345–4359.
30. Giles J (2005) The dustiest place on Earth. *Nature* 434:816–819.
31. Washington R, et al. (2006) Links between topography, wind, deflation, lakes and dust: The case of the Bodélé Depression, Chad. *Geophys Res Lett* 33:L09401.
32. Washington R, Todd MC, Engelstaedter S, M'Bainayel S, Mitchell F (2006) Dust and the low-level circulation over the Bodélé Depression, Chad: Observations from BoDEx 2005. *J Geophys Res* 111:D03201.
33. Schepanski K, Tegen I, Laurent B, Heinold B, Macke (2007) A new Saharan dust source activation frequency map derived from MSG-SEVIRI IR-channels. *Geophys Res Lett* 34:L18803.
34. Todd MC, et al. (2007) Mineral dust emission from the Bodélé Depression, northern Chad, during BoDEx 2005. *J Geophys Res* 112:D06207.
35. Knippertz P, Fink AH (2006) Synoptic and dynamic aspects of an extreme springtime Saharan dust outbreak. *Q J R Meteorol Soc* 132:1153–1177.
36. Cotton WR, et al. (2003) RAMS 2001: Current status and future directions. *Meteorol Atmos Phys* 82:5–29.
37. Cautenet G, et al. (2000) Modelling a Saharan dust event. *Meteorol Z* 9:221–230.
38. Bouet C, et al. (2007) Mesoscale modeling of aeolian dust emission during the BoDEx 2005 experiment. *Geophys Res Lett* 34:L07812.
39. Marticorena B, Bergametti G (1995) Modeling the atmospheric dust cycle 1. Design of a soil-derived dust emission scheme. *J Geophys Res* 100:16415–16430.
40. Marticorena B, et al. (1997) Modeling the atmospheric dust cycle 2. Simulations of Saharan dust sources. *J Geophys Res* 102:4287–4404.
41. Legrand M, Plana-Fattori A, N'Doume C (2001) Satellite detection of dust using the IR imagery of Meteosat 1. Infrared Difference Dust Index. *J Geophys Res* 106:18251–18274.
42. Servant M, Servant S (1983) Paleolimnology of an upper quaternary endorheic lake in Chad basin. *Monographiae Biologicae* 53:11–26.
43. Schuster M, et al. (2003) Coastal conglomerates around Hadjer el Khamis inselbergs (western Chad, central Africa): New evidence for Lake Mega-Chad episodes. *Earth Surf Proc Land* 28:1059–1069.
44. Formenti P, Elbert W, Maenhaut W, Haywood J, Andreae MO (2003) Chemical composition of mineral dust aerosol during the Saharan Dust Experiment (SHADE) airborne campaign in the Cape Verde region, September 2000. *J Geophys Res* 108:8576.
45. Chiapello I, et al. (1997) Origins of African dust transported over the northeastern tropical Atlantic. *J Geophys Res* 102:13701–13709.
46. Moreno T, et al. (2006) Geochemical variations in aeolian mineral particles from the Sahara-Sahel dust corridor. *Chemosphere* 65:261–270.
47. Schluter T (2006). *Geological Atlas of Africa*, (Springer, Berlin), pp 152–154.
48. Engelstaedter S, Washington R (2007) Atmospheric controls on the annual cycle of North African dust. *J Geophys Res* 112:D03103.
49. Martin JH, Fitzwater SE (1988) Iron deficiency limits phytoplankton growth in the north-east Pacific subarctic. *Nature* 331:341–343.
50. Measures CI, Landing WM, Brown MT, Buck CS (2008) High-resolution AL and Fe data from the Atlantic Ocean CLIVAR-CO2 repeat hydrography A16N transect: Extensive linkages between atmospheric dust and upper ocean geochemistry. *Global Biogeochem Cycles* 22:GB1005.
51. Blain S, et al. (2004) Availability of iron and major nutrients for phytoplankton in the northeast Atlantic Ocean, Limmol. *Oceanography* 49:2095–2104.
52. Mills MM, Ridame C, Davey M, LaRoche J, Geider RJ (2004) Iron and phosphorus co-limit nitrogen fixation in the eastern tropical North Atlantic. *Nature* 429:292–294.
53. Garrison VH, et al. (2003) African and Asian dust: From desert soils to coral reefs. *Bioscience* 53:469–480.
54. Hoerling M, Hurrell J, Eischeid J, Phillips A (2006) Detection and attribution of twentieth-century northern and southern African rainfall change. *J Clim* 19:3989–4008.
55. Cook KH, Vizy EK (2006) Coupled model simulations of the West African Monsoon system: Twentieth- and twenty-first century simulations. *J Clim* 19:3681–3703.